BOLETÍN DE LA SOCIEDAD ESPAÑOLA DE

Cerámica y Vidrio

Thermoelectric doping effect in Ca$_3$Co$_{4-x}$Ni$_x$O$_9$ ceramics

CrossMark

Gabriel Constantinescu[a], Shahed Rasekh[b], Miguel Angel Torres[b], Pablo Bosque[c], Maria Antonieta Madre[b], Andres Sotelo[b], and Juan Carlos Diez[b,]*

[a] *National Institute of Materials Physics, Magurele, Bucharest, Romania*
[b] *Instituto de Ciencia de Materiales de Aragón (Zaragoza University-Consejo Superior de Investigaciones Científicas), Zaragoza, Spain*
[c] *University Center for the Defense of Zaragoza, General Military Academy, Zaragoza, Spain*

ARTICLE INFO

ABSTRACT

Ca$_3$Co$_{4-x}$Ni$_x$O$_9$ (x=0.01, 0.03, and 0.05) polycrystalline thermoelectric ceramics have been prepared by the classical solid state method. As a result of the Ni addition an increase in porosity has been detected. Moreover, the presence of Ni has been related with the increase of Ca$_2$Co$_3$O$_6$ secondary phase and the appearance of a new NiO-CoO solid solution.

However, for the 0.01-Ni doped samples an improvement in the thermoelectric performances has been measured. This effect has been related with a decrease in the resistivity values and an increase in the Seebeck coefficient.

The raise in the power factor for the 0.01-Ni doped samples, compared with the undoped ones, is between 10 and 25% at 50 and 800 °C respectively. Moreover, the maximum power at 800 °C, around 0.25 mW/K^2.m, is significantly higher than the best results obtained in Ni doped samples reported previously in the literature.

Efecto del dopaje en la propiedades termoeléctricas de cerámicas Ca$_3$Co$_{4-x}$Ni$_x$O$_9$

RESUMEN

Se han preparado muestras policristalinas de Ca$_3$Co$_{4-x}$Ni$_x$O$_9$ (x = 0,01, 0,03 y 0,05) mediante reacción en estado sólido. Se ha detectado un incremento de la porosidad en las muestras dopadas con Ni. La adición de Ni también ha provocado el aumento de la fase secundaria Ca$_2$Co$_3$O$_6$, así como la aparición de una nueva fase consistente en una solución sólida de NiO-CoO.

A pesar de ello se ha detectado una mejora de las prestaciones termoeléctricas en las muestras con un 0,01 de Ni. Esta mejora ha sido provocada por una disminución de la resistividad eléctrica y un aumento del coeficiente Seebeck.

* Corresponding author.
E-mail address: monux@unizar.es (J.C. Diez).

Se ha encontrado que el factor de potencia de las muestras con un 0,01 de Ni es un 10% superior a T ambiente y un 25% superior a 800 °C que el encontrado en muestras sin dopar. Por otra parte, el valor del factor de potencia medido a 800 °C, aproximadamente 0,25 mW/K^2.m, es significativamente más alto que los valores que se pueden encontrar en la literatura para muestras dopadas con Ni.

Introduction

Thermoelectric materials (TE) are receiving ongoing interest as they can harvest wasted heat from many different energy transforming processes. Furthermore, these materials can directly transform a temperature gradient into electrical power, without moving parts, due to the well-known Seebeck effect. The conversion efficiency of TE materials is usually quantified using the figure of merit $ZT=TS^2/\rho\kappa$, where S is Seebeck coefficient, ρ electrical resistivity, κ thermal conductivity, and T is the absolute temperature.[1] When only the electrical part of this expression is considered (S^2/ρ), it is called power factor (PF) which is often used to characterise the materials performances when the thermal conductivity is difficult to be measured.

Intermetallic materials are currently employed in several practical applications, as energy harvesters. However, due to their chemical degradation and/or oxidation at high temperature under oxidative conditions, they have problems when used in these conditions. On the other hand, these types of materials are often composed of heavy, scarce, and toxic elements, as Te, Sb, etc. The working temperature limitation of these materials was surpassed by discovery of high TE performances in the Na-Co-O ceramic system.[2] Thenceforth many works have been performed on the cobalt-based ceramics for high temperature applications, mainly on the $Ca_3Co_4O_9$,[3,4] $Bi_2Sr_2Co_2O_x$,[5,6] $Bi_2Ca_2Co_2O_x$,[7,8] and $Bi_2Ba_2Co_2O_x$[9,10] systems with high thermoelectric properties and working temperatures.

Crystallographic studies performed on these cobalt-based materials have demonstrated that they can be described by a monoclinic structure which is, in turn, composed of two stacked alternating layers: a conductive CdI_2-type hexagonal CoO_2 layer with a two-dimensional triangular lattice, and an insulating rock-salt-type (RS). Both sublattices possess common a- and c-axis lattice parameters and β angles, but different b-axis length which produces a misfit along the b-direction.[11] Moreover, the high structural anisotropy of these materials leads to the formation of plate-like grains with very large dimensions in the ab plane and very small ones in the c direction. As a consequence, this effect can be taken in advantage to preferentially align these grains to obtain bulk properties close to those obtained in single crystals. There are many techniques that have been tested in order to produce well aligned grains in bulk Co-based materials, as hot uniaxial pressing,[12] spark plasma sintering,[13] laser floating zone melting (LFZ),[14] electrically assisted laser floating zone,[15] etc. The main disadvantages of these methods are due to different factors, as the relatively long treatments, the high costs associated with the processes and/or the strong dependence on the growth or the texturing speed.[12,13,16,17]

Moreover, previous works have demonstrated that the Seebeck coefficient values are influenced by changes in the incommensurability ratio and/or the effective charge of the RS block layer between the CoO_2 ones.[18] These studies have supplied the basis for the TE properties modification using cationic substitution. The most common ones are based on the substitution of an alkaline-earth,[19,20] Co,[21,22] or Pb[23,24] which have been effective in improving the materials performances.

The aim of this work is studying the effect of small substitutions of Co by Ni on the structural, microstructural, and high temperature thermoelectric properties of $Ca_3Co_{4-x}Ni_xO_9$ when it is prepared using a classical solid state synthesis route.

Experimental

$Ca_3Co_{4-x}Ni_xO_9$ polycrystalline ceramic materials, with x=0.00, 0.01, 0.03, and 0.05, were prepared using commercial $CaCO_3$ (Panreac, 98+%), Co_2O_3 (Aldrich, 98+%), and NiO (Aldrich, 99%) powders as starting materials by the classical solid state route. They were weighed in the appropriate proportions, mixed and ball milled for 30 minutes in acetone media at 300 rpm, in a RESTH® S100 ball mill. The resulting suspension has been heated with infrared radiation to evaporate the acetone. The dry mixture was subsequently manually milled and thermally treated for 12 h at 750 and 800 °C, under air, with an intermediate manual grinding. This thermal treatment has been found in previous works to be adequate to decompose the $CaCO_3$.[25] After the thermal treatment, the powders were uniaxially pressed at 400 MPa for 1 minute in form of parallelepipeds (approximately 3 mmx3 mmx14 mm) and sintered at 900 °C in air for 24 h with a final furnace cooling.

Powder X-ray diffraction (XRD) patterns have been recorded in order to identify the different phases in the thermoelectric sintered materials. Data have been collected at room temperature, with 2θ ranging between 5 and 60 degrees, using a Rigaku D/max-B X-ray powder diffractometer working with Cu Kα radiation.

Microstructural observations were performed on polished longitudinal sections of the samples, using a Field Emission

Scanning Electron Microscope (FESEM, Carl Zeiss Merlin) fitted with an energy dispersive X-ray spectrometer (EDX). Micrographs of the samples have been used to analyse the different phases and their distribution. Apparent density measurements have been performed on several samples for each composition after sintering, using 4.677 g/cm³ as theoretical density.[26] Oxygen content was determined by means of cerimetric titrations as described previously in detail.[27]

Electrical resistivity and Seebeck coefficient were simultaneously determined by the standard dc four-probe technique in a LSR-3 measurement system (Linseis GmbH), in the steady state mode and at temperatures ranging from 50 to 800 °C under He atmosphere. Moreover, with the electrical resistivity and Seebeck data, the power factor has been calculated in order to determine the samples performances. These properties have been compared with the results obtained in the undoped samples and with those reported in the literature at room temperature ($\cong$50 °C), where oxygen diffusion is negligible, to avoid the influence of the atmosphere on the compared values.

Results and discussion

Powder XRD patterns for the different $Ca_3Co_{4-x}Ni_xO_9$ samples are displayed in Figure 1 (from 5 to 40° for clarity). From these data, it is clear that all the samples have very similar diffrac-

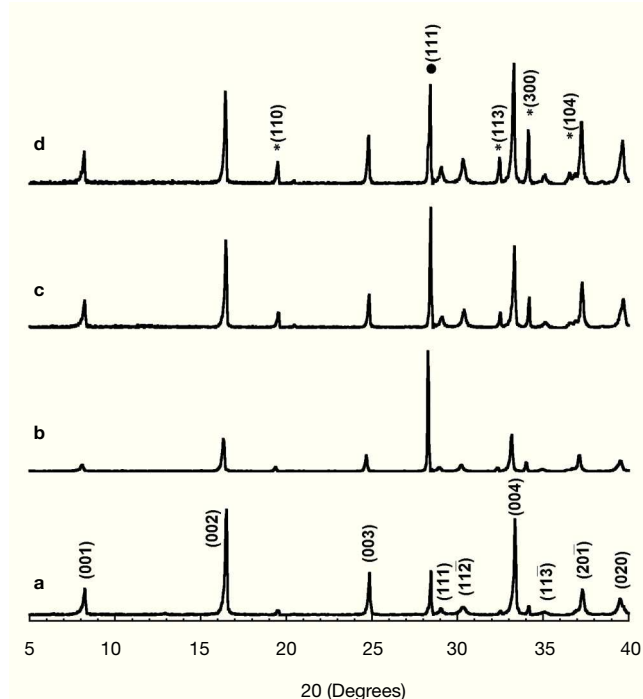**Figure 1 – Powder XRD patterns of $Ca_3Co_{4-x}Ni_xO_9$ samples, with x=0.00 (a), 0.01 (b), 0.03 (c), and 0.05 (d). The diffraction planes indicate the $Ca_3Co_4O_9$ phase and the * the $Ca_3Co_2O_6$ ones. The reflection plane marked with • belongs to Si (used as internal reference).**

tion patterns. As can be seen in Figure 1a, corresponding to the undoped samples, the highest peaks have been associated to the thermoelectric $Ca_3Co_4O_9$ phase, indicated by the reflection planes, in agreement with previously reported data,[28] where a monoclinic unit cell (#12, C12/m1) has been used. On the other hand, the peak at around 28.65 degrees (indicated by • in Figure 1d) corresponds to the (111) diffraction plane of Si used as reference. Moreover, the peaks identified by * (see Figure 1d), have been associated to the $Ca_3Co_2O_6$ phase, in agreement with previously reported data,[29] with a rhombohedral unit cell (#167, R$\bar{3}$cH). From these data, it seems that a slight increase in the amount of the $Ca_3Co_2O_6$ phase can be found with Ni addition. The most evident differences between the XRD patterns obtained for all samples are due to the preferential orientation of the plate-like grains. These changes in the preferential orientation lead to the observed variation in the relative intensities between the different crystallographic planes. This is a typical effect associated with the preparation of powdered samples when they are composed of very anisotropic grains (as plate-like ones) which can induce different preferential grain orientations in the powders. On the other hand, the volume of the thermoelectric phase has remained unchanged, about 236±0.5 Å³, when evaluated with the help of FullProf software.

General SEM observations performed on representative longitudinal polished sections of the $Ca_3Co_{4-x}Ni_xO_9$ samples are shown in Figure 2. In these images, it can be observed that all samples possess very similar microstructure, indicating that Ni doping does not greatly influence the samples microstructure. As it can be easily seen in Figure 2, all the Ni-doped samples present a relatively high degree of porosity, indicated by the black contrast, which seems to increase from the 0.01 to the 0.03 and 0.05 Ni-doped samples. In order to confirm this observation, apparent density measurements have been performed for all samples. At least four samples for each composition were measured for three times to minimize measurement errors. These results have shown that Ni-doped samples possess densities between $\cong$64% (for the 0.01 Ni-doped samples) and $\cong$62% (for the 0.03 and 0.05% Ni-doped samples) of ρ_{th} with a mean standard error of ±0.02 in all cases, which are significantly lower than the values obtained for the undoped samples ($\cong$72% of ρ_{th}), indicating that small additions of nickel are worsening the densification process. The presence of this porosity is due to relatively low thermal stability of the $Ca_3Co_4O_9$ phase (maximum stability temperature $\cong$926 °C), compared with the minimum temperature to produce the liquid phase ($\cong$1350 °C).[30] The great difference between both temperatures leads to a very slow densification process at the sintering temperature (900 °C), explaining the relatively high porosity obtained in these samples.[4]

The EDX analysis has shown that all the samples are mainly composed by $Ca_3Co_4O_9$ with some small amounts of $Ca_3Co_2O_6$. The substituted nickel has not been detected in none of the doped samples, in neither of the Ca-Co-O phases. On the other hand, the EDX analysis detected the Ni in a NiO-CoO solid solution (visible in Figures 2b-2d as the small areas of bright-grey contrast), of variable composition, in all the doped samples. The presence of this new phase could be explained by the total solubility between the CoO and NiO
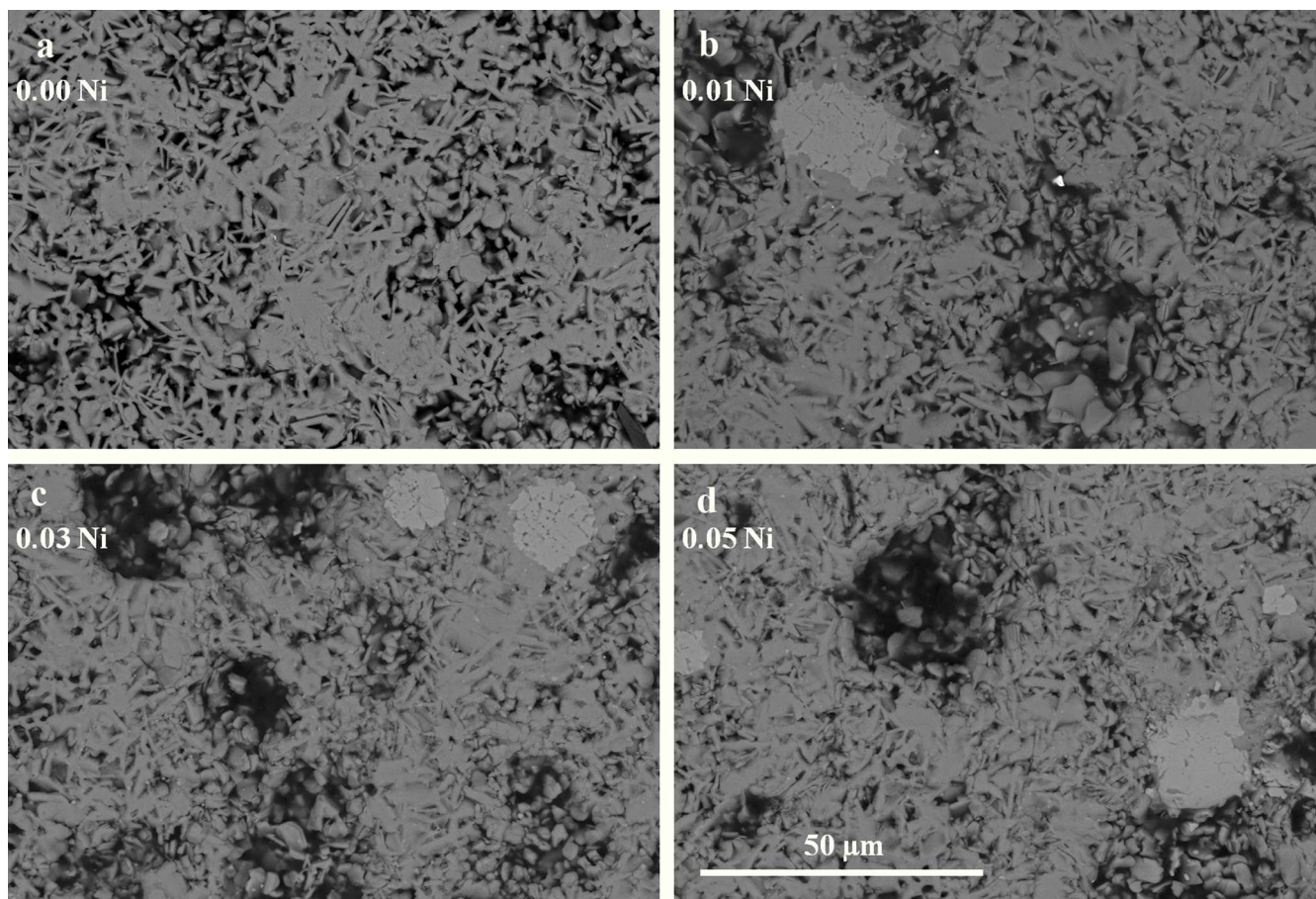
Figure 2 – SEM micrographs performed on representative longitudinal polished sections of $Ca_3Co_{4-x}Ni_xO_9$ samples, for x=0.00 (a); 0.01 (b), 0.03 (c), and 0.05 (d).

at the sintering temperatures used in this study, as can be deduced from the equilibrium phase diagram of the NiO-CoO system.[31] In principle, the SEM-EDX results are in agreement with the powder XRD ones discussed previously, except for the NiO-CoO solid solutions which were not detected in the powder XRD diffractograms, probably due to the their small amounts.

The variation of the Seebeck coefficient or thermopower with the temperature for all the Ni-doped samples can be seen in Figure 3. In the plot, it can be clearly seen that the sign of the thermopower is positive in the entire measured temperature range, which confirms a conduction mechanism mainly governed by holes. The values of the Seebeck coefficient for all the samples increase almost linearly with temperature. This fact can be associated with a typical behaviour of metallic compound or a semiconductor in the saturation region.[32] On the other hand, the values of the Seebeck coefficient for all the Ni-doped samples are slightly higher than of the undoped one. The obtained values at room temperature, between 135 and 140 µV/K, are slightly higher than those reported elsewhere ($\cong$110 µV/K) at the same temperature for Ni-doped samples.[22] Moreover, the maximum Seebeck coefficient value ($\cong$215 µV/K) obtained in this work at 800 °C is

significantly higher than the obtained previously in Ni-doped samples ($\cong$180 µV/K).[22] Furthermore, these higher S values for all the Ni-doped samples could be attributed to a lower concentration of Co^{4+} ions in the conductive CdI_2-type layers of the $Ca_3Co_4O_9$ compound, as given by the modified Heikes formula.[33] In order to check this assumption, the mean cobalt valence, calculated using cerimetric titrations has been used. The results have shown that the mean cobalt valence from the 0.01 ($\cong$3.06), 0.03 ($\cong$3.09), and 0.05 ($\cong$3.08) Ni-doped samples are lower than the one of the undoped ones ($\cong$3.11), indicating lower Co^{4+} concentrations and consequently higher thermopower values.[33]

On the other hand, the S values obtained in this work for the undoped samples at room temperature ($\cong$135 µV/K) are higher than other values found in literature, for sinter-forged $Ca_3Co_4O_9$ samples ($\cong$120 µV/K) prepared by solid-state reactions, at the same temperature,[34] for undoped $Ca_3Co_4O_9$ samples ($\cong$120 µV/K) synthesized by a cold high-pressure method, at room temperature,[35] or for other undoped $Ca_3Co_4O_9$ samples ($\cong$125 µV/K), at the same temperature.[36,37]

The temperature dependence of the electrical resistivity of the different Ni-doped samples is presented in Figure 4. In this graph, it can be easily seen that all the resistivity curves

show a semiconducting-like behaviour (dρ/dT<0), from room temperature to around 400 °C, followed by a metallic-like one (dρ/dT>0) at higher temperatures. As it was previously reported for this type of materials, the charge transport process in the semiconducting regime is represented by a thermally-activated hole hopping mechanism from Co^{4+} to Co^{3+},[38] while in the metallic one the charge carriers are transported in the valence o conduction bands.[22] Taking into account the high porosity of the samples, these resistivity values could be considered as relatively low. Moreover, the porosity and the formation of the non-thermolectric (Co,Ni) O solid solutions can explain the increase of the resistivity values for the 0.03 and 0.05 Ni-substituted samples. In any case, the lowest resistivity values, obtained for the 0.01 Ni-substituted samples (between 17 and 19 mΩ.cm) are around the best values found for undoped $Ca_3Co_4O_9$ samples prepared by spark plasma sintering (13 mΩ.cm),[13] and slightly lower than the obtained for the Ni-doped ones (20 mΩ.cm).[22]

To better clarify the resistivity behaviour, the activation energy values for the different samples were calculated in the semiconducting regime. The energy activation value found for the 0.01-Ni sample, 34 meV, was lower than the value found for the undoped samples, 36 meV. As a consequence, and in spite of the lower density and secondary non TE phases found in the 0.01 sample, the resistivity values are lower in the high temperature region. The activation energy values found for the 0.03-Ni sample (34 meV) and 0.05-Ni one (43 meV), together with the higher amount of porosity and secondary phases, explain the higher resistivity values found for these Ni-substituted samples, as compared with the undoped one.
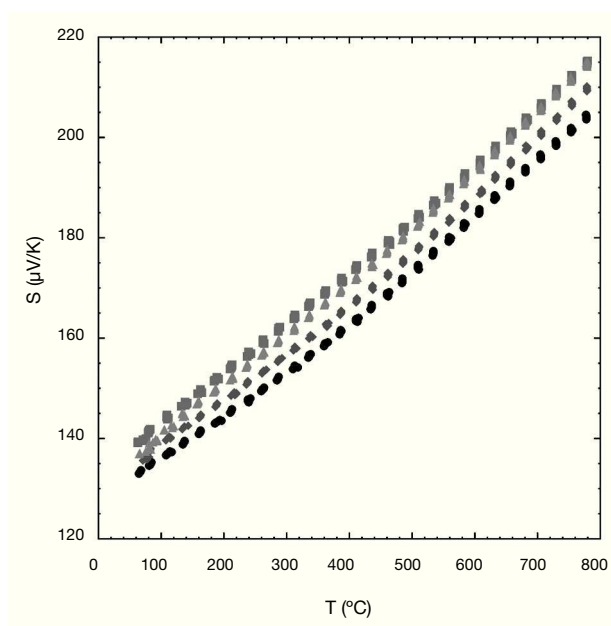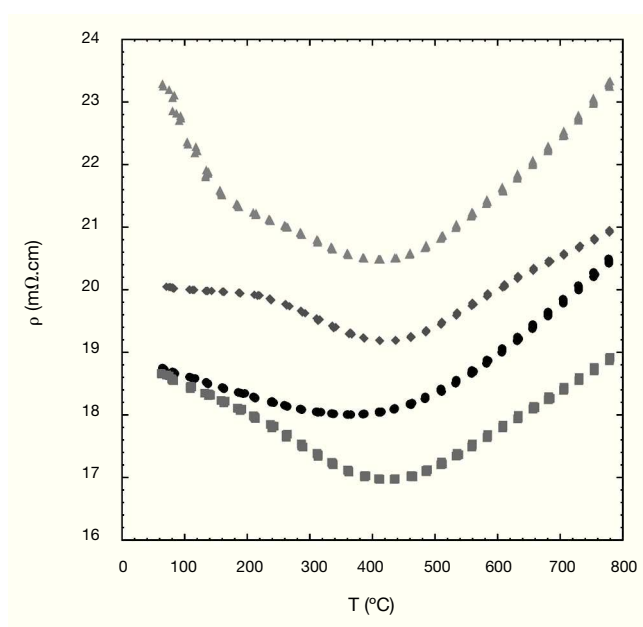

Figure 4 – Temperature dependence of the electrical resistivity, as a function of Ni content, in Ca$_3$Co$_{4-x}$Ni$_x$O$_9$ samples, for x=0.00 (●); 0.01 (■); 0.03 (♦); and 0.05 (▲).

In order to evaluate the thermoelectric performances of these materials, the power factor has been calculated using the electrical resistivity and Seebeck coefficient data and plotted as a function of temperature in Figure 5. When considering PF values at about 50 °C ($\cong$ room temperature), it can be clearly seen that the 0.01 Ni-doped samples possess higher PF values than the undoped ones (around 10%). The highest PF value obtained at 800 °C (around 0.25 mW/K^2.m) for the 0.01 Ni-doped samples is $\cong$25% higher than the obtained for the undoped samples. This maximum PF value is around 90% higher than the obtained in Ni substituted samples prepared by a sol-gel method ($\cong$0.13 mW/K^2.m at 700 °C)[22] which is known for producing higher quality samples than the classical solid state method.

All these data indicate that very small Ni additions are adequate to improve, in a significant manner, the thermoelectric performances of $Ca_3Co_4O_9$ ceramics, when they are properly processed.

Conclusions

This paper demonstrates that very small Ni substitutions for Co in $Ca_3Co_4O_9$ thermoelectric ceramics improve its performances by increasing the Seebeck coefficient values and by decreasing the electrical resistivity. The optimal Ni for Co substitution has been determined using the power factor values at 50 and 800 °C, which are maximum for the 0.01 Ni-doped samples. The raise in PF, compared with the undoped samples, is between 10 and 25% at 50 and 800 °C respectively. Moreover, the measured PF values at 800 °C are about 90%
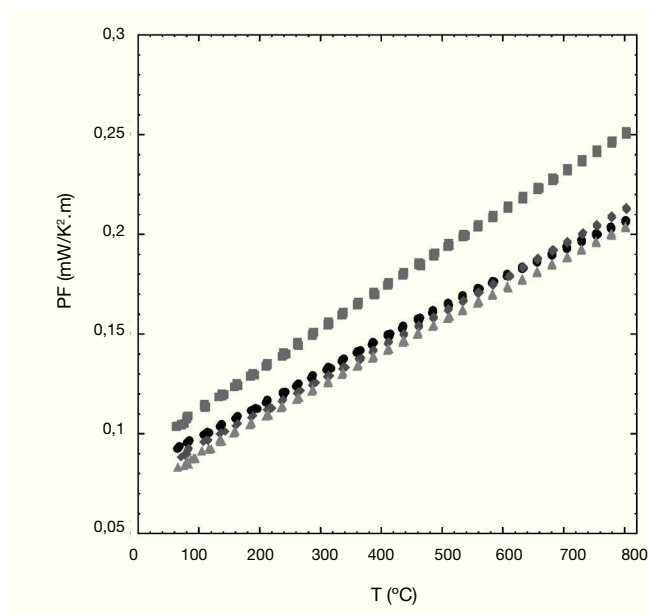

Figure 3 – Temperature dependence of the Seebeck coefficient, as a function of Ni content, in Ca$_3$Co$_{4-x}$Ni$_x$O$_9$ samples, for x=0.00 (●); 0.01 (■); 0.03 (♦); and 0.05 (▲).

Figure 5 – Temperature dependence of the power factor, as a function of Ni content, in $Ca_3Co_{4-x}Ni_xO_9$ samples, for x=0.00 (●); 0.01 (■); 0.03 (♦); and 0.05 (▲).

higher than the best Ni doped ones reported in the literature prepared by sol-gel method which provides highly homogeneous materials.

Acknowledgements

REFERENCES

1. Rowe, D. M. (2006): General Principles and Basic Considerations. In Rowe, D. M. (2006) (ed.), *Thermoelectrics handbook: macro to nano*, CRC Press, Boca Raton, FL, USA, pp. 1-10.
2. Terasaki, I.; Sasago, Y.; Uchinokura, K.; (1997): Large thermoelectric power in $NaCo_2O_4$ single crystals. *Phys. Rev. B* 56 (20), 12685-12687. http://dx.doi.org/10.1103/PhysRevB.56. R12685.
3. Huang, Y.; Zhao, B.; Fang, J.; Ang, R.; Sun, Y.; (2011): Tunning of microstructure and thermoelectric properties of $Ca_3Co_4O_9$ ceramics by high-magnetic-field sintering. *J. Appl. Phys.* 110 (12), 123713. http://dx.doi.org/10.1063/1.3671403.
4. Sotelo, A.; Constantinescu, G.; Rasekh, Sh.; Torres, M. A.; Diez, J. C.; Madre, M. A.; (2012): Improvement of thermoelectric properties of $Ca_3Co_4O_9$ using soft chemistry synthetic methods. *J. Eur. Ceram. Soc.* 32 (10), 2415-2422. http://dx.doi. org/10.1016/j.jeurceramsoc.2012.02.012.
5. Rubesova, K.; Hlasek, T.; Jakes, V.; Huber, S.; Hejtmanek, J.; Sedmidubsky, D.; (2015): Effect of a powder compaction process on the thermoelectric properties of $Bi_2Sr_2Co_{1.8}O_x$ ceramics. *J. Eur. Ceram. Soc.* 35 (2), 525-531. http://dx.doi.org/10.1016/j. jeurceramsoc.2014.08.037.
6. Diez, J. C.; Guilmeau, E.; Madre, M. A.; Marinel, S.; Lemmonier, S.; Sotelo, A.; (2009): Improvement of $Bi_2Sr_2Co_{1.8}O_x$ thermoelectric properties by laser floating zone texturing. *Solid State Ionics* 180 (11-13), 827-830. http://dx.doi.org/10.1016/j.ssi.2009.02.004.
7. Sun, N.; Dong, S. T.; Zhang, B. B.; Chen, Y. B.; Zhou, J.; Zhang, S. T.; Gu, Z. B.; Yao, S. H.; Chen, Y. F.; (2013): Intrinsically modified thermoelectric performance of alkaline-earth isovalently substituted $[Bi_2 AE _2O_4][CoO_2]_y$ single crystals. *J. Appl. Phys.* 114 (4), 043705. http://dx.doi.org/10.1063/1.4816315.
8. Sotelo, A.; Guilmeau, E.; Rasekh, Sh.; Madre, M. A., Marinel, S.; Diez, J. C.; (2010): Enhancement of the thermoelectric properties of directionally grown Bi–Ca-Co-O through Pb for Bi substitution. *J. Eur. Ceram. Soc.* 30, 1815-1820. http://dx.doi. org/10.1016/j.jeurceramsoc.2010.01.037.
9. Ang, R.; Sun, Y. P.; Luo, X.; Song, W. H.; (2007): A narrow band contribution with Anderson localization in Ag-doped layered cobaltites $Bi_2Ba_3Co_2O_y$. *J. Appl. Phys.* 102 (7), 073721. http:// dx.doi.org/10.1063/1.2795622.
10. Rasekh, Sh.; Constantinescu, G.; Torres, M. A.; Madre, M. A.; Diez, J. C.; Sotelo, A.; (2012): Growth rate effect on microstructure and thermoelectric properties of melt grown $Bi_2Ba_2Co_2O_x$ textured ceramics. *Adv. Appl. Ceram.* 111 (8), 490-494. http://dx.doi.org/10.1179/1743676112Y.0000000039.
11. Miyazaki, Y.; (2004): Crystal structure and thermoelectric properties of the misfit-layered cobalt oxides. *Solid State Ionics* 172 (1-4), 463-467. http://dx.doi.org/10.1016/j.ssi.2004.01.046.
12. Wang, H.; Sun, X.; Yan, X.; Huo, D.; Li, X.; Li, J.-G.; Ding, X.; (2014): Fabrication and thermoelectric properties of highly textured $Ca_9Co_{12}O_{28}$ ceramic. *J. Alloys Compds.* 582, 294-298. http://dx.doi.org/10.1016/j.jallcom.2013.07.145.
13. Butt, S.; Liu, Y.-C.; Lan, J.-L.; Shehzad, K.; Zhan, B.; Lin, Y.; Nan, C.-W.; (2014): High-temperature thermoelectric properties of La and Fe co-doped Ca-Co-O misfit-layered cobaltites consolidated by spark plasma sintering. *J. Alloys Compds.* 588, 277-283. http://dx.doi.org/10.1016/j.jallcom.2013.11.098.
14. Sotelo, A.; Guilmeau, E.; Madre, M. A.; Marinel, S.; Lemmonier, S.; Diez, J. C.; (2008): $Bi_2Ca_2Co_{1.7}O_x$ thermoelectric ceramics textured by laser floating zone method. *Bol. Soc. Esp. Ceram. V.* 47 (4), 225-228.
15. Ferreira, N. M.; Rasekh, Sh.; Costa, F. M.; Madre, M. A.; Sotelo, A.; Diez, J.C.; Torres, M. A.; (2012): New method to improve the grain alignment and performance of thermoelectric ceramics. *Mater. Lett.* 83, 144-147. http://dx.doi.org/10.1016/j. matlet.2012.05.131.
16. Diez, J. C.; Rasekh, Sh.; Madre, M. A.; Guilmeau, E.; Marinel, S.; Sotelo, A.; (2010): Improved Thermoelectric Properties of Bi-M-Co-O (M = Sr, Ca) Misfit Compounds by Laser Directional Solidification. *J. Electron. Mater.* 39, 1601-1605. http://dx.doi. org/10.1007/s11664-010-1232-2.
17. Constantinescu, G.; Rasekh, Sh.; Torres, M. A.; Madre, M. A.; Diez, J. C.; Sotelo, A.; (2013): Enhancement of the high-temperature thermoelectric performance of $Bi_2Ba_2Co_2O_x$ ceramics. *Scripta Mater.* 68 (1), 75-78. http://dx.doi.org/10.1016/j. scriptamat.2012.09.014.
18. Maignan, A.; Pelloquin, D.; Hébert, S.; Klein, Y.; Hervieu, M.; (2006): Thermoelectric Power In Misfit Cobaltites Ceramics: Optimization by Chemical Substitutions. *Bol. Soc. Esp. Ceram. V.* 45 (3) , 122-125. http://dx.doi.org/10.3989/cyv.2006.v45.i3.290.

19. Constantinescu, G.; Rasekh, Sh.; Torres, M. A.; Diez, J. C.; Madre, M. A.; Sotelo, A.; (2013): Effect of Sr substitution for Ca on the $Ca_3Co_4O_9$ thermoelectric properties. *J. Alloys Compds.* 577, 511-515. http://dx.doi.org/10.1016/j.jallcom.2013.07.005.

20. Abdellahi, M.; Bahmanpour, M.; Bahmanpour, M.; (2015): Modeling Seebeck coefficient of $Ca_{3-x}M_xCo_4O_9$ (M=Sr, Pr, Ga, Ca, Ba, La, Ag) thermoelectric ceramics. *Ceram. Int.* 41 (1), 345-352. http://dx.doi.org/10.1016/j.ceramint.2014.08.077.

21. Diez, J. C.; Torres, M. A.; Rasekh, Sh.; Constantinescu, G.; Madre, M. A. ; Sotelo, A.; (2013): Enhancement of $Ca_3Co_4O_9$ thermoelectric properties by Cr for Co substitution. *Ceram. Int.* 39 (6) , 6051-6056. http://dx.doi.org/10.1016/j.ceramint.2013.01.021.

22. Pinitsoontorn, S.; Lerssongkram, N.; Keawprak, N.; Amornkitbamrung, V.; (2012): Thermoelectric properties of transition metals-doped $Ca_3Co_{3.8}M_{0.2}O_{9+\delta}$ (M = Co, Cr, Fe, Ni, Cu and Zn). *J. Mater. Sci.: Mater. Electron.* 23, 1050-1056. http://dx.doi.org/10.1007/s10854-011-0546-z.

23. Sotelo, A. ; Rasekh, Sh.; Guilmeau, E. ; Madre, M. A.; Torres, M. A.; Marinel, S.; Diez, J. C.; (2011): Improved thermoelectric properties in directionally grown $Bi_2Sr_2Co_{1.8}O_y$ ceramics by Pb for Bi substitution. *Mater. Res. Bull.* 46 (12), 2537-2542. http://dx.doi.org/10.1016/j.materresbull.2011.08.011.

24. Liu, J. ; Yang, H. S. ; Chai, Y. S.; Zhu, L.; Qu, H. ; Sun, C. H.; Gao, H. X. ; Chen, X. D.; Ruan, K. Q.; Cao, L. Z.; (2006): Study on the anomalous thermopower and resistivity of (Bi, Pb)-Sr-Co-O: Evidence of a narrow band contribution with Anderson localization. *Phys. Lett. A* 356 (1), 85-88. http://dx.doi.org/10.1016/j.physleta.2006.03.016.

25. Sotelo, A.; Sh. Rasekh, Sh.; Madre, M. A.; E. Guilmeau, E.; Marinel, S. ; Diez, J. C.; (2011): Solution-based synthesis routes to thermoelectric $Bi_2Ca_2Co_{1.7}O_x$. *J. Eur. Ceram. Soc.* 31 (9), 1763-1769 (2011). http://dx.doi.org/10.1016/j.jeurceramsoc.2011.03.008.

26. Masset, A. C.; Michel, C.; Maignan, A.; Hervieu, M.; Toulemonde, O.; Studer, F.; Raveau, B.; Hejtmanek, J.; (2000): Misfit-layered cobaltite with an anisotropic giant magnetoresistance: Ca3Co4O9. *Phys. Rev. B* 62 (1), 166-175. http://dx.doi.org/10.1103/PhysRevB.62.166.

27. Madre, M. A.; Costa, F. M.; Ferreira, N. M.; Sotelo, A.; Torres, M. A.; Constantinescu, G.; Rasekh, Sh.; Diez, J. C.; (2013): Preparation of high-performance $Ca_3Co_4O_9$ thermoelectric ceramics produced by a new two-step method. *J. Eur. Ceram. Soc.* 33, 1747 (2013). http://dx.doi.org/10.1016/j.jeurceramsoc.2013.01.029.

28. Kajitani, T.; Yubuta, K.; Huang, X. Y.; Miyazaki, Y.; (2009): Discommensuration of Doped $[Ca_2CoO_3]_p$ CoO_2. *J. Electron. Mater.* 38 (7), 1462-1467. http://dx.doi.org/10.1007/s11664-009-0784-5.

29. Hervoches, C. H.; Okamoto, H.; Kjekshus, A. ; Fjellvag, H.; Hauback, B.; (2009): Crystal structure and magnetic properties of the solid-solution phase $Ca_3Co_{2-v}Mn_vO_6$. *J. Solid State Chem.* 182 (2), 331-338. http://dx.doi.org/10.1016/j.jssc.2008.10.016.

30. Woermann, E.; Muan, A.; (1970): Phase equilibria in the system CaO-cobalt oxide in air. *J. Inorg. Nucl. Chem.* 32 (5), 1455-1459. http://dx.doi.org/10.1016/0022-1902(70)80631-5.

31. Kinoshita, M.; Kingery, W.D.; Bowen, H.K.; (1973): Phase Separation in NiO-CoO Solid Solution Single Crystals. *J. Am. Ceram. Soc.* 56 (7), 398-399. http://dx.doi.org/10.1111/j.1151-2916.1973.tb12703.x.

32. Ioffe, A.F. (1960): *Physics of semiconductors*, Academic Press, New York, USA.

33. Koshibae, W.; Tsutsui, K.; Maekawa, S.; (2000): Thermopower in cobalt oxides. *Phys. Rev. B* 62 (11), 6869-6872. http://dx.doi.org/10.1103/PhysRevB.62.6869.

34. Prevel, M.; Perez, O.; Noudem, J.G.; (2007): Bulk textured $Ca_{2.5}(RE)_{0.5}Co_4O_9$ (RE: Pr, Nd, Eu, Dy and Yb) thermoelectric oxides by sinter-forging. *Solid State Sci.* 9 (3-4), 231-235. http://dx.doi.org/10.1016/j.solidstatesciences.2007.01.003.

35. Wang, Y.; Sui, Y.; Wang, X.; Su, W.; Liu, X.; (2010): Enhanced high temperature thermoelectric characteristics of transition metals doped $Ca_3Co_4O_{9+\delta}$ by cold high-pressure fabrication. *J. Appl. Phys.* 107, 033708. http://dx.doi.org/10.1063/1.3291125.

36. Wang, Y.; Sui, Y.; Ren, P.; Wang, L.; Wang, X.; Su, W.; Fan, H.; (2010): Strongly Correlated Properties and Enhanced Thermoelectric Response in $Ca_3Co_{4-x}M_xO_9$ (M = Fe, Mn, and Cu). *Chem. Mater.* 22 (3), 1155-1163. http://dx.doi.org/10.1021/cm902483a.

37. Li, D.; Qin, X.Y.; Gu, Y.J. ; Zhang, J.; (2005): The effect of Mn substitution on thermoelectric properties of $Ca_3Mn_xCo_{4-x}O_9$ at low temperatures. *Solid State Commun.* 134 (4), 235-238. http://dx.doi.org/10.1016/j.ssc.2005.01.044.

38. Lin, Y. H.; Lan, J.; Shen, Z. J.; Liu, Y. H.; Nan, C. W.; Li, J. F.; (2009): High-temperature electrical transport behaviors in textured $Ca_3Co_4O_9$-based polycrystalline ceramics. *Appl. Phys. Lett.* 94 (7), 072107. http://dx.doi.org/10.1063/1.3086875.